

Dual attenuation factor in nanographene molecular wires

Sara Sangtarash

School of Engineering, University of Warwick, CV4 7AL Coventry, United Kingdom

sara.sangtarash@warwick.ac.uk

Designing molecular nanowires with high electrical conductance that facilitate efficient charge transport over long distances are highly desirable for future molecular-scale circuitry. However most of the molecular wires act as tunnel barriers and their electrical conductance is decaying exponentially with increasing the length. Just recently a few studies have shown increasing conductance with length. In this study, for the first time, we have identified new class of molecular wires that exhibit both increase and decrease of room temperature conductance with length (dual attenuation factor) depend on their connection points to electrodes. We show that this dual attenuation factor is an inherent property of these graphene-like nanowires and its demonstration depends on the constructive quantum interference pattern for different connectivities to electrode. This is significant because a given nanographene molecular wire can show both negative and positive attenuation factor. This enables a systematic design of connectivity dependent high/low-conductance molecular wires for future molecular-scale circuitry.

Understanding electron transport in molecular junctions, identifying length dependence and long-range charge transport across individual molecules are important for the advancement of molecular electronics.¹⁻⁵ While a wide variety of molecular nanowires have been studied for many years, most of them typically act as tunnel barriers and their conductance (G) decays exponentially by molecular length (L) as $G = Ae^{-\beta L}$ where A is prefactor and β is the decay (attenuation) factor.^{6,7} This exponential decay in conductance with the wire length severely limit their applications for future molecular-scale circuitry. For example, conjugated molecular wires such as oligophenylene⁸ show conductance values decay with increasing number of phenyl units to the extent of $\beta = 0.41 \text{ \AA}^{-1}$, for oligo(phenylene-ethynylenes) OPEs, measured room-temperature values of β range from $0.2\text{--}0.34 \text{ \AA}^{-1}$,⁹ 0.33 \AA^{-1} for oligo(aryleneethynylenes) OAEs.¹⁰ Other molecular wire such as oligophenyleneimine¹¹, oligonaphthalene fluoreneimine¹² and alkanedithiol⁷ showed attenuation factors of 0.3 \AA^{-1} , 0.25 \AA^{-1} and 0.9 \AA^{-1} respectively. Recently there has been growing interest in the design of molecular nanowires with an increasing conductance with length, called negative attenuation (β) molecular wires. As an example, negative β has been demonstrated in the cumulene and fused porphyrin molecular wires¹³⁻²⁰.

In the molecular structure studied today, a particular molecular wire either shows a positive or negative attenuation factor. In this paper for the first time, we have identified new class of nanographene molecular wires where a given molecular wire shows both positive and negative attenuation factor (dual attenuation factor or DAF) depending on the connection point to electrode. This connectivity dependent DAF arises from the room temperature quantum interference in the multipath nanographene structures. In what follows, we will first demonstrate the DAF effect using simple tight binding method^{21,22} and confirm it using the material specific first principle calculations.

Figure 1A shows the molecular junction formed from a nanographene molecular core connected to electrodes from two different connections e.g. (i,j) and (i,k). To simplify the notation, we use blue connectivity for i,j connectivity to electrodes and red connectivity for i,k connectivity to electrodes. The nanographene molecular wire (NMW) consists of a naphthalene unit (n in Fig 1A) connected to the neighboring naphthalene to form wires with different lengths. We first construct the tight-binding Hamiltonian of these structures with length $n=1$ to $n=20$ naphthalene units using $\epsilon=0\text{eV}$ for on-site energies and $\gamma=-2.7\text{eV}$ for coupling integrals between neighboring sites²³. We then calculate transmission coefficient of electrons with energy E passing from one electrode to the other through molecule connected to electrodes from blue and red connectivities. The conductance can then be calculated from Landauer formula $G = G_0 T(E_F)$ where G_0 is conductance quantum and E_F is the Fermi energy of electrodes.

Our calculation shows that depend on the connection point to the electrodes, the conductance of NMW increases (negative attenuation factor) or decreases (positive attenuation factor) with length. For junctions formed through the red connectivity (Fig. 1), the conductance decreases by the length of NMW around $E=0\text{eV}$ in Fig. 2A. In contrast, the conductance surprisingly increases by the length of NMW around $E=0\text{eV}$ for NMW with the blue connectivity to electrodes as shown in Fig. 2B leading to a negative attenuation factor. The positive and negative attenuation factor is an intrinsic property of NMW, which arises from the constructive quantum interference (CQI) pattern in this molecular core. This result is very significant because it shows a given molecular wire can exhibit conventional behavior (decrease of conductance with length) if connected through one (e.g. red) connectivity but surprisingly different behavior (increase of conductance with length) by connecting it to electrode through another (e.g. blue) connectivity.

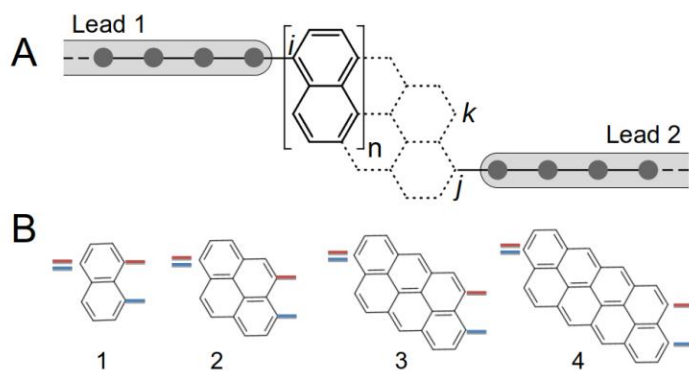


Figure 1: Molecular structure of naphthalene molecular wire (NMW). A) NMW between two 1D electrodes, B) Examples of the NMW with length 1 to 4. The red and blue lines represent the connection points to the electrodes.

Figure 2C shows the changes of transmission for molecular wire shown in Fig. 1A for lengths up to 20 naphthalene units ($n=20$). The red (blue) curve represents changes of transmission coefficient for red (blue) connectivities to electrode. Clearly, the conductance increase rapidly initially and then saturates for blue connectivity whereas it decays for red connectivity.

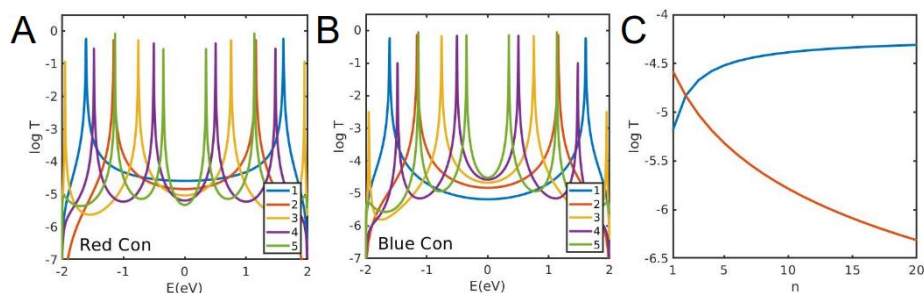


Figure 2: Tight-binding transmission coefficient T . A) and B) Transmission coefficient of red and blue connectivities of the molecules 1- 5 respectively (structures shown in Figure 1). C) Transmission coefficient versus length of NMW at $E=0$ eV demonstrating dual beta factor in NMW junctions.

To confirm this result obtained from simple tight binding model that considers the contribution of pi orbitals only, we have also performed material specific calculations using density functional theory (DFT) obtained material specific Hamiltonian of junctions formed by the NMW core 1-5 (see Fig. 1) connected to two gold electrodes through thiol anchors and acetylene linkers. Figs. 3A and 3C show examples of such junctions for NMW with length 5 naphthalene units. We then calculate transmission coefficient of electrons with energy E traversing from right gold electrode to the left one using our quantum transport code Gollum²⁴. Fig. 3B and 3D show the corresponding transmission coefficient for two different connectivities and the same molecular core versus different lengths. For connection similar to the blue connectivity in Fig. 1, DFT transmission calculations show very

similar behaviour where the conductance increases with length from 1 to 5 (Figure 3B). Crucially, this happens for all energies between the HOMO and LUMO gaps, confirming the robustness of the negative attenuation factor effect in these junctions. In contrast, when the same molecular core is connected through the red connectivity (similar to the red connectivity in Fig. 1), the conductance decreases with length from 1 to 5 for a wide range of energies around the DFT Fermi energy ($E=0$). These material specific calculations confirm the DAF effect in these molecular cores.

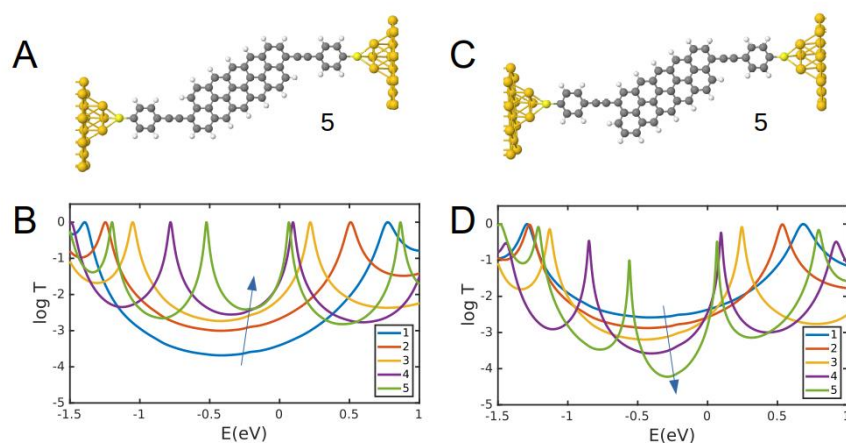


Figure 3: Transmission coefficient from material specific DFT-NEGF calculations. A) and C) Example of junctions formed using NMW core with length 5 connected to gold electrodes through thiol anchors and acetylene linkers. B) and D) Transmission coefficient for junctions with NMW cores and connectivities shown in A and C, respectively with lengths between 1-5.

To further investigate if DAF is unique only for the red and blue connectivities, we performed tight-binding calculations with other connectivities as shown in Fig. 4A. We found that similar behaviour is observed for connectivities shown with green and orange colours in Fig. 4A. Fig. 4B shows the transmission coefficient through molecules 1-4 connected from green connectivity to electrodes. The conductance decreases with length around $E=0$ eV for this connectivity. In contrast, the conductance increases with length when the molecule connected to electrodes through orange connectivity (Fig. 4C). Similar to red and blue connectivities (Fig. 2C) of NMW to electrodes, the electron transmission at $E = 0$ eV increases rapidly with length initially and then saturates for the NMW with orange connectivity to electrodes whereas it decays by length for the green connectivity.

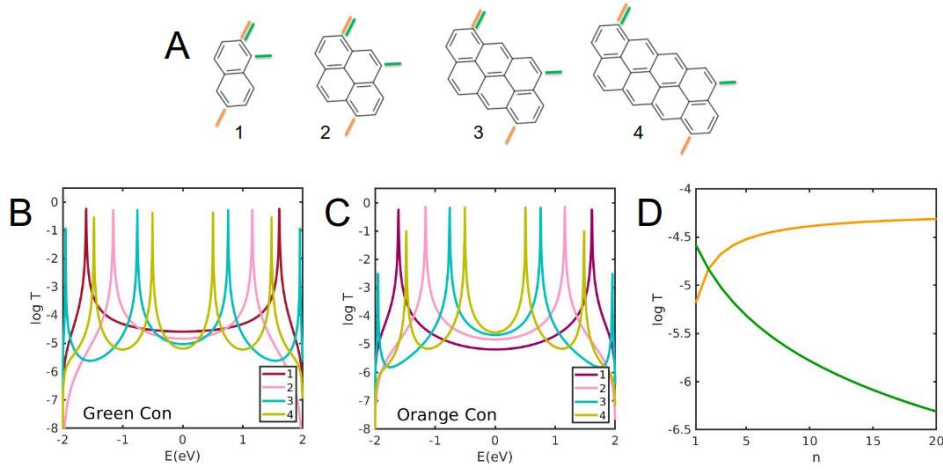


Figure 4: NMW with another set of connectivities to electrodes. A) Molecular structures and connection points (green and orange) to electrodes for NMWs with length 1 to 4. B) and C) Transmission coefficient of the molecular wires with green and orange connectivities, respectively from length 1-4. D) Transmission coefficient versus length of NMW at $E=0$ eV demonstrating dual beta factor in NMW junctions with green and orange connection points to electrodes.

In summary, we demonstrated that a given molecular core e.g. NMW can exhibit two different attenuation factors depend on the connection point to electrodes and the constructive quantum interference pattern formed. We call this DAF effect and demonstrate it by a simple tight binding model as well as material specific DFT-NEGF calculations. This enables a systematic design of connectivity dependent high/low-conductance molecular wires for future molecular-scale circuitry.

Theoretical methods

The Hamiltonian of the structures described in Figure 2 and 4 was constructed from a tight-binding approximation with a single orbital per atom of site energy $\epsilon = 0$ for carbon and nearest-neighbor couplings $\gamma = -2.6$ for both C—C bonds.

Geometry optimization: The geometry of structures shown in Figure 3 was relaxed to the force tolerance of 10 meV/Å using the *SIESTA*²⁵ implementation of density functional theory (DFT), with a double- ζ polarized basis set (DZP) and the Local Density Approximation (LDA) functional with CA parameterization. A real-space grid was defined with an equivalent energy cut-off of 250 Ry.

Transport Calculation: A simple tight-binding Hamiltonian or mean-field Hamiltonian H obtained from the converged DFT calculation were combined with our implementation of the nonequilibrium Green's function method, Gollum,²⁶ to calculate the phase-coherent, elastic scattering properties of each system consist of left (source) and right (drain) leads and the scattering region (molecule). The transmission coefficient²⁷ $T(E)$ for electrons of energy E (passing from the source to the drain) is calculated via the relation $T(E) = \text{Trace}(\Gamma_R(E)G^R(E)\Gamma_L(E)G^{R\dagger}(E))$. In this expression, $\Gamma_{L,R}(E) = i(\Sigma_{L,R}(E) - \Sigma_{L,R}^\dagger(E))$ describe the level broadening due to the coupling between left (L) and right (R) electrodes and the central scattering region, $\Sigma_{L,R}(E)$ are the retarded self-energies associated with this coupling and $G^R = (ES - H - \Sigma_L - \Sigma_R)^{-1}$ is the retarded Green's function, where H is the Hamiltonian and S is the overlap matrix.

Electrical conductance: Using the obtained transmission coefficient ($T(E)$), the conductance could be calculated by the Landauer formula ($G = G_0 \int dE T(E)(-\partial f / \partial E)$) where $G_0 = 2e^2/h$ is the conductance quantum, $f(E) = (1 +$

$\exp((E - E_F)/k_B T))^{-1}$ is the Fermi-Dirac distribution function, T is the temperature and $k_B = 8.6 \times 10^{-5}$ eV/K is the Boltzmann's constant.

Acknowledgements

The author acknowledges the Leverhulme Trust for Early Career Fellowship no. ECF-2018-375.

Conflicts of interest

There are no conflicts to declare.

References

- (1) Sangtarash, S.; Vezzoli, A.; Sadeghi, H.; Ferri, N.; Brien, H. M. O.; Grace, I.; Higgins, S. J.; Nichols, R. J.; Lambert, C. J. Gateway State-Mediated, Long-Range Tunnelling in Molecular Wires †‡. **2018**, *18*, 3060–3067. <https://doi.org/10.1039/c7nr07243k>.
- (2) Datta, S.; van Houten, H. *Electronic Transport in Mesoscopic Systems*; Cambridge Univ Pr, 1996; Vol. 49. <https://doi.org/10.1063/1.2807624>.
- (3) Sadeghi, H.; Sangtarash, S.; Lambert, C. Robust Molecular Anchoring to Graphene Electrodes. 31–34.
- (4) Sedghi, G.; Sawada, K.; Esdaile, L. J.; Hoffmann, M.; Anderson, H. L.; Bethell, D.; Haiss, W.; Higgins, S. J.; Nichols, R. J. Single Molecule Conductance of Porphyrin Wires with Ultralow Attenuation. *J. Am. Chem. Soc.* **2008**, *130* (27), 8582–8583. <https://doi.org/10.1021/ja802281c>.
- (5) Ferreira, Q.; Bragança, A. M.; Alcácer, L.; Morgado, J. Conductance of Well-Defined Porphyrin Self-Assembled Molecular Wires up to 14 Nm in Length. *J. Phys. Chem. C* **2014**, *118* (13), 7229–7234. <https://doi.org/10.1021/jp501122n>.
- (6) Sadeghi, H. Theory of Electron, Phonon and Spin Transport in Nanoscale Quantum Devices. *Nanotechnology* **2018**, *29* (37), 373001. <https://doi.org/10.1088/1361-6528/aace21>.
- (7) Sangtarash, S.; Vezzoli, A.; Sadeghi, H.; Ferri, N.; O'Brien, H. M.; Grace, I.; Bouffier, L.; Higgins, S. J.; Nichols, R. J.; Lambert, C. J. Gateway State-Mediated, Long-Range Tunnelling in Molecular Wires. *Nanoscale* **2018**, *10* (6), 3060–3067. <https://doi.org/10.1039/C7NR07243K>.
- (8) Wold, D. J.; Haag, R.; Rampi, M. A.; Frisbie, C. D. Distance Dependence of Electron Tunneling through Self-Assembled Monolayers Measured by Conducting Probe Atomic Force Microscopy: Unsaturated versus Saturated Molecular Junctions. *J. Phys. Chem. B* **2002**, *106* (11), 2813–2816. <https://doi.org/10.1021/jp013476t>.
- (9) Lambert, C. J.; Wandlowski, T. Correlations between Molecular Structure and Single-Junction Conductance: A Case Study with Oligo(Phenylene-Ethynylene)-Type Wires. **2012**. <https://doi.org/10.1021/ja211555x>.
- (10) Zhao, X.; Huang, C.; Gulcur, M.; Batsanov, A. S.; Baghernejad, M.; Hong, W.; Bryce, M. R.; Wandlowski, T. Oligo(Aryleneethynylene)s with Terminal Pyridyl Groups: Synthesis and Length Dependence of the Tunneling-to-Hopping Transition of Single-Molecule Conductances. *Chem. Mater.* **2013**, *25* (21), 4340–4347. <https://doi.org/10.1021/cm4029484>.
- (11) Seong, H. C.; Kim, B.; Frisbie, C. D. Electrical Resistance of Long Conjugated Molecular Wires. *Science* **2008**, *320* (5882), 1482–1486. <https://doi.org/10.1126/science.1156538>.
- (12) Choi, S. H.; Risko, C.; Carmen Ruiz Delgado, M.; Kim, B.; Brédas, J. L.; Daniel Frisbie, C. Transition from Tunneling to Hopping Transport in Long, Conjugated Oligo-Imine Wires Connected to Metals. *J. Am. Chem. Soc.* **2010**, *132* (12), 4358–4368. <https://doi.org/10.1021/ja910547c>.
- (13) Tada, T.; Yoshizawa, K. Reverse Exponential Decay of Electrical Transmission in Nanosized Graphite Sheets. *J. Phys. Chem. B* **2004**, *108* (23), 7565–7572. <https://doi.org/10.1021/jp0310908>.
- (14) Ramos-Berdullas, N.; Mandado, M. Electronic Properties of P-Xylylene and P-Phenylene Chains Subjected to Finite Bias Voltages: A New Highly Conducting Oligophenyl Structure. *Chem. Eur. J.* **2013**, *19* (11), 3646–3654.
- (15) Li, S.; Gan, C. K.; Son, Y.-W.; Feng, Y. P.; Quek, S. Y. Anomalous Length-Independent Frontier Resonant Transmission Peaks in Armchair Graphene Nanoribbon Molecular Wires. *Carbon N. Y.* **2014**, *76*, 285–291.
- (16) Tsuji, Y.; Movassagh, R.; Datta, S.; Hoffmann, R. Exponential Attenuation of Through-Bond Transmission in a Polyene: Theory and Potential Realizations. *ACS Nano* **2015**, *9* (11), 11109–11120. <https://doi.org/10.1021/acs.nano.5b04615>.
- (17) Stuyver, T.; Fias, S.; De Proft, F.; Geerlings, P. The Relation between Delocalization, Long Bond Order Structure Count and Transmission: An Application to Molecular Wires. *Chem. Phys. Lett.* **2015**, *630*, 51–56. <https://doi.org/10.1016/j.cplett.2015.04.043>.

- (18) Algethami, N.; Sadeghi, H.; Sangtarash, S.; Lambert, C. J. The Conductance of Porphyrin-Based Molecular Nanowires Increases with Length. 1–8.
- (19) Garner, M. H.; Bro-Jørgensen, W.; Pedersen, P. D.; Solomon, G. C. Reverse Bond-Length Alternation in Cumulenes: Candidates for Increasing Electronic Transmission with Length. *J. Phys. Chem. C* **2018**, *122* (47), 26777–26789. <https://doi.org/10.1021/acs.jpcc.8b05661>.
- (20) Leary, E.; Limburg, B.; Alanazy, A.; Sangtarash, S.; Grace, I.; Swada, K.; Esdaile, L. J.; Noori, M.; Gonza, M. T.; Rubio-bollinger, G.; Higgins, S. J.; Lambert, C. J.; Sadeghi, H.; Hodgson, A.; Anderson, H. L.; Nichols, R. J. *Bias-Driven Conductance Increase with Length in Porphyrin Tapes*; 2018. <https://doi.org/10.1021/jacs.8b06338>.
- (21) Sangtarash, S.; Huang, C.; Sadeghi, H.; Sorohhov, G.; Hauser, J. Searching the Hearts of Graphene-like Molecules for Simplicity, Sensitivity, and Logic. **2015**. <https://doi.org/10.1021/jacs.5b06558>.
- (22) Geng, Y.; Sangtarash, S.; Huang, C.; Sadeghi, H.; Fu, Y.; Hong, W.; Wandlowski, T.; Decurtins, S.; Lambert, C.; Liu, S. Magic Ratios for Connectivity-Driven Electrical Conductance of Graphene-like Molecules .
- (23) Reich, S.; Maultzsch, J.; Thomsen, C.; Ordejón, P. Tight-Binding Description of Graphene. *Phys. Rev. B - Condens. Matter Mater. Phys.* **2002**. <https://doi.org/10.1103/PhysRevB.66.035412>.
- (24) Ferrer, J.; Lambert, C. J.; García-Suárez, V. M.; Manrique, D. Z.; Visontai, D.; Oroszlany, L.; Rodríguez-Ferradás, R.; Grace, I.; Bailey, S. W. D.; Gillemot, K.; Sadeghi, H.; Algharagholy, L. A. GOLLUM: A next-Generation Simulation Tool for Electron, Thermal and Spin Transport. *New J. Phys.* **2014**, *16*, 093029. <https://doi.org/10.1088/1367-2630/16/9/093029>.
- (25) Soler, J. M.; Artacho, E.; Gale, J. D.; García, A.; Junquera, J.; Ordejón, P.; Sánchez-Portal, D. The SIESTA Method for Ab Initio Order- N Materials Simulation. *J. Phys. Condens. Matter* **2002**, *14* (11), 2745–2779. <https://doi.org/10.1088/0953-8984/14/11/302>.
- (26) Ferrer, J.; Lambert, C. J.; Manrique, D. Z. GOLLUM : A next-Generation Simulation Tool for Electron , Thermal and Spin Transport. **2014**, *16*. <https://doi.org/10.1088/1367-2630/16/9/093029>.
- (27) Sadeghi, H. Theory of Electron , Phonon and Spin Transport. **2018**, *29* (37), 1–30. <https://doi.org/10.1088/1361-6528/aace21>.